The Role of MR and CT in Evaluating Clival Chordomas and Chondrosarcomas

Robert F. Oot[1,2]
Gordon E. Melville[1,3]
Paul F. J. New[1]
Mary Austin-Seymour[4]
John Munzenrider[4]
John Pile-Spellman[1]
Marie Spagnoli[1,5]
Gregory M. Shoukimas[1,6]
K. Jack Momose[1]
Roberta Carroll[1,7]
Kenneth R. Davis[1]

Sixteen chordomas and nine chondrosarcomas of the clivus were evaluated with CT and MR either before (22 cases) or after (three cases) treatment with proton beam irradiation. The ability of these imaging techniques to provide information necessary to direct patient treatment was studied. The tumor was detected and its gross margins were identified by both techniques in all instances. No reliable diagnostic features allowing differentiation between these two tumors were encountered. MR generally was superior in defining the exact position of the brainstem and optic chiasm relative to the tumor, and it frequently provided superior information about tumor extension into the nasopharynx and cavernous sinus. CT was always better than MR in demonstrating tumoral calcification and in defining the exact anatomy of bone destruction. MR was generally superior to CT in demonstrating the position of the cavernous internal carotid artery relative to the tumor and often provided superior visualization of the vertebral and basilar arteries. In cases in which bone-induced artifact obscured the interface between the neural axis and tumor in the CT image, or in which the tumor had suprasellar extension and was likely to compress the optic chiasm and tracts, MR was of great value in planning irradiation therapy. The high occurrence of clinically asymptomatic signal intensity alterations in the MR studies of previously treated patients appears to limit the differential diagnostic value of this information.

Given its greater availability and lower cost, CT appears to be the technique of choice for routine follow-up of previously treated patients.

This article appears in the July/August 1988 issue of *AJNR* and the September 1988 issue of *AJR*.

Received May 14, 1986; accepted after revision January 6, 1988.

Presented at the annual meeting of the American Society of Neuroradiology, San Diego, January 1986.

[1] Department of Radiology, Massachusetts General Hospital and the Harvard Medical School, Boston, MA 02114.

[2] Present address: Department of Radiology, Nashua Memorial Hospital, 8 Prospect St., Nashua, NH 03061. Address reprint requests to R. F. Oot.

[3] Present address: Somerset Medical Center, Somerville, NJ 08876.

[4] Department of Radiation Therapy, Massachusetts General Hospital, Boston, MA 02114.

[5] Present address: St. Lukes Hospital, Utica, NY 13503.

[6] Present address: West Suburban Imaging Center, Wellesley, MA 02181.

[7] Present address: Department of Radiology, Beth Israel Hospital, New York, NY 10003.

***AJNR* 9:715–723, July/August 1988**
0195–6108/88/0904–0715

Chordomas are rare, slow-growing neoplasms that arise from remnants of the notochord. Approximately 35–40% of these tumors occur intracranially, where they typically involve the clivus [1–3]. While these tumors rarely metastasize to distant sites, they are locally aggressive, and total surgical resection is generally impossible [4–6]. Recently, proton beam therapy has been used to treat these difficult lesions with extremely encouraging results, suggesting that this may be the definitive treatment for such tumors [7, 8]. Identical therapy has also been used at this institution, with equal success, to treat low-grade chondrosarcomas of the clivus and adjacent skull base.

It is crucial that the tumor volume and its relationship to adjacent neural structures be defined accurately both before radiation therapy and in following patients' response to treatment. We report on the relative capabilities of MR and CT in providing this and other information required to direct treatment in a series of 16 chordomas and nine low-grade chondrosarcomas of the clivus and adjacent skull base.

Subjects and Methods

Sixteen patients with chordoma, including one chondroid subtype tumor, and nine patients with low-grade chondrosarcoma were studied. The patients included 12 males and 13 females, ranging in age from 7–79 years. Twenty-two patients were imaged before proton beam irradiation, 2 to 12 months after surgical biopsy and/or debulking of the tumor. Three patients had undergone both surgical biopsy and proton beam irradiation 2 to 5 years earlier and had been treated with dosages of from 66.6 to 73.5 cobalt gray equivalents.

All CT studies were performed on third- or fourth-generation scanners. Axial IV contrast-enhanced scans were obtained in all patients. In seven cases unenhanced scans were also obtained, while in eight cases direct coronal imaging was also performed. In four of 16 patients, CT was performed after the lumbar subarachnoid administration of metrizimide (4–6 ml of 170 mg I/ml).

MR was performed using a whole-body system operating at 0.6 T. Almost all scans were performed with a 28.5-cm-diameter head coil. Multislice technique was performed. Slice thickness was 5 or 7 mm. Image acquisition was obtained by using 128 phase encoding (y axis) steps, with interpolation to 256 for image display. In the x axis, 256 frequency points were displayed, for a total display matrix of 256 × 256. Spatial resolution was 1.0 × 2.0 mm. Both T1- and T2-weighted images were obtained in all patients. T1-weighted images were obtained by using spin echo sequences with 400–500/22–30 (TR range/TE range) or inversion recovery sequences with 1450–1500/450–500/30–32 (TR range/TI range/TE range). T2-weighted images were obtained by using dual spin echo sequences with 2000/60, 120 (TR/first-echo TE, second-echo TE). Almost all patients underwent axial T2-weighted (23/25) and sagittal T1-weighted (18/25) sequences.

Results

The tumor was identified by both CT and MR in all patients. The CT examination revealed the bulk of the tumor to be of increased density, relative to the adjacent neural axis, in all but one case. Enhancement was seen in every instance in which both plain and IV contrast-enhanced scans were available (Fig. 1). The CT appearance of one chordoma was atypical, showing marked hypodensity, with contrast enhancement limited to the dura adjacent to the tumor (Fig. 2). Evidence of destruction of the clivus was present in all cases. Frequently, bone destruction of the skull base was extensive. Tumoral calcification and/or the presence of bone sequestra were demonstrated in 17 patients.

MR showed the bulk of the tumor to have prolonged T1 and T2 relaxation in all instances. While T1 and T2 values were not calculated, there was no visible difference in signal intensity between lesions that had been exposed to radiotherapy and tumors that had not yet been treated. We were unable to differentiate between chordoma and chondrosarcoma on the basis of signal intensity characteristics. The one case of chondroid chordoma did not have a different appearance. In 13 of 25 cases, the tumor had a homogeneous appearance (Fig. 1). In the remaining 12 patients, significant heterogeneity was detected. Foci of postsurgical fat packing were detected in four patients, and in five patients areas of shortened T1 and prolonged T2 relaxation times, thought to most likely represent old hemorrhage, were identified. In eight patients, calcification was depicted as foci of decreased or absent signal.

While the gross tumor margins were well seen by both imaging techniques in all cases, the relative capabilities of MR and CT in defining the exact relationship between tumor and adjacent structures are summarized in Table 1. MR provided better delineation of the posterior margin of the tumor and its relationship to the brainstem than did CT in 18 of 25 patients. While both CT and MR demonstrated abnormal findings in the 20 patients with tumor involving the cavernous sinus region (Fig. 3), MR was equal or superior to CT in demonstrating this finding in all but one case. While the superior border of the tumor was accurately depicted by both CT and MR in

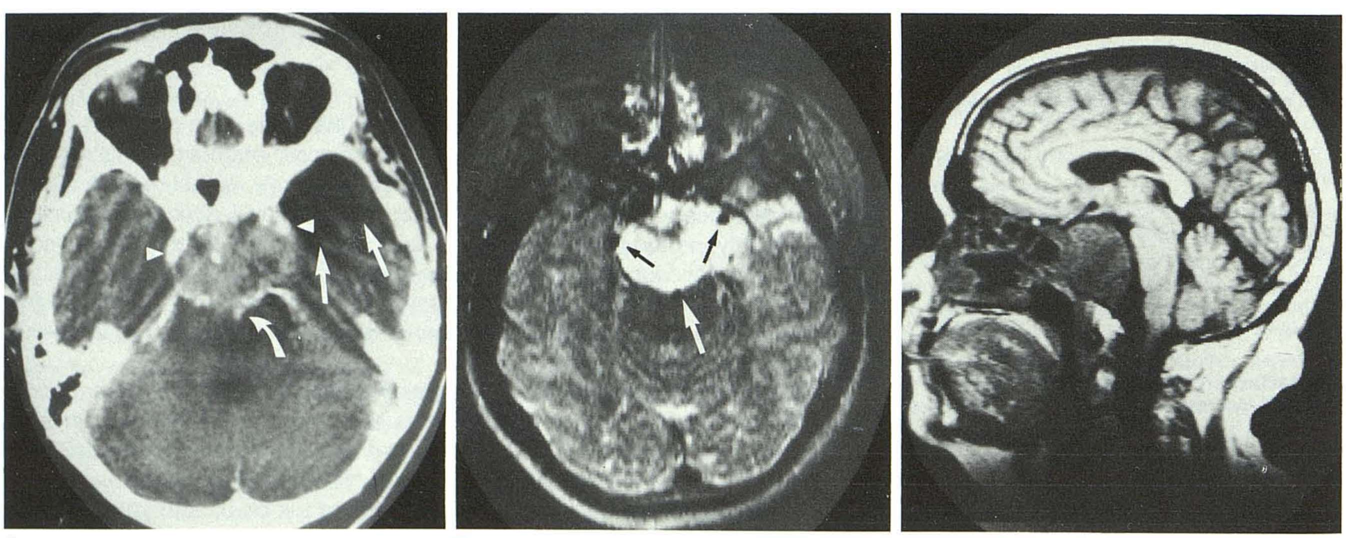

A B C

Fig. 1.—Chordoma in 54-year-old woman.

A, Axial postcontrast CT scan. Large, high-density tumor mass, deforming and displacing brainstem posteriorly. Basilar artery (*curved arrow*) and cavernous internal carotid arteries (*arrowheads*) are identifiable. Tissue loss from a previous partial temporal lobectomy is clearly shown (*straight arrows*).

B, Axial SE 2000/(60),*120 MR image. Bulk of tumor demonstrates prolonged T2 relaxation time. Positions of both carotid arteries (*black arrows*) and basilar artery (*white arrow*) can be discriminated as flow voids.

C, Sagittal 500/30 MR image shows that tumor has prolonged T1 relaxation. Note replacement of normal clival marrow by tumor.

*** The echo time not in parentheses is illustrated.**

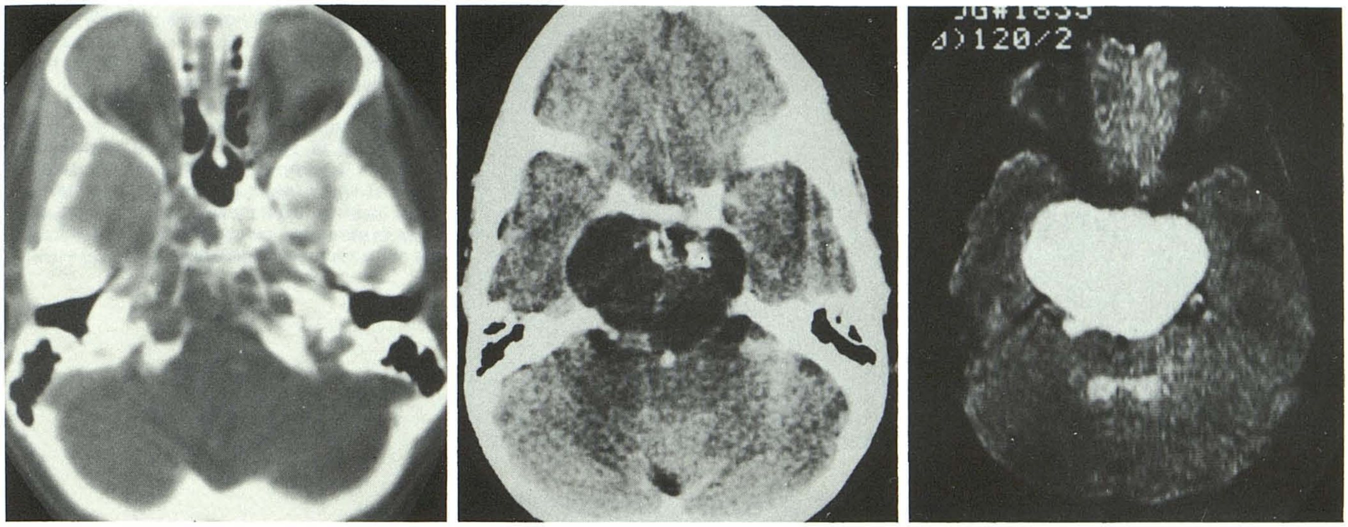

A B C

Fig. 2.—Chordoma in 7-year-old boy. At surgery, the tumor was solid and was interpreted pathologically as chordoma, with some features suggesting a cartilaginous component. Tumor did not invade the dura.

***A* and *B*, Axial postcontrast CT scans show that tumor is of low density, associated with extensive bone destruction.**

***C*, Axial SE 2000/(60),120 MR image shows that tumor has very prolonged T2 relaxation time and homogeneous appearance.**

TABLE 1: Relative Capabilities of CT and MR in Tumor Staging

	MR > CT	MR = CT	CT > MR
Posterior margin of tumor	18/25	7/25	—
Cavernous sinus extension[a]	7/20	12/20	1/20
Superior margin of tumor	7/9	2/9	—
Nasopharyngeal tumor	2/4	2/4	—

[a] Includes both tumor extending into cavernous sinus as well as outward compression without invasion.

the nine patients in whom suprasellar extension had occurred, MR provided superior information in seven of nine cases, generally because it better demonstrated the position of the optic chiasm relative to the tumor. MR was always equal or superior to CT in defining nasopharyngeal extension of the tumor, which occurred in six patients (Fig. 4).

T1 weighted images were generally most useful in defining tumor margins relative to adjacent CSF. In contrast, T2-weighted images usually proved superior in separating tumor from anatomically contiguous neural structures and the normal nasopharynx. The anterior margin of the tumor, when in close apposition to mucoid material in the nasal cavity and paranasal sinuses, could be more difficult to define accurately. In many, but not all, instances, the tumor appeared to be of lower signal intensity than adjacent mucous on T1-weighted images and of equal or higher signal intensity on T2-weighted images.

MR proved superior to CT in demonstrating the position of the internal carotid arteries, relative to the tumor, in 16 of 20 patients in whom tumor involved the cavernous sinus region (Fig. 5). In the remaining four cases, the two imaging techniques were judged to be equally accurate. By MR, the vessels were reliably seen as flow voids whereas it was generally difficult to differentiate the enhancing artery from the high-density and/or enhancement of the tumor and normal cavernous sinus. In all patients, both internal carotid arteries were seen as flow voids by MR and were usually displaced by the tumor. In three patients, MR clearly showed tumor surrounding and encasing an internal carotid artery, which appeared to be narrowed in two instances. In contrast, the position of the vertebral and basilar arteries could usually be accurately determined by IV contrast-enhanced CT, and the two imaging techniques were judged to provide equivalent information in 15 of 25 cases. In nine of 25 patients, however, MR was judged superior to CT in defining these vascular relationships, largely because of bone-induced artifacts in the CT image that obscured the vessels. In only one instance was CT judged superior to MR in the delineation of these posterior fossa vessels.

MR and CT differed significantly in their respective ability to depict changes associated with previous surgery. CT was invariably more accurate in the depiction of postsurgical bone changes. Of the 11 patients who had undergone temporal or temporoparietal craniotomies and who had not received previous radiation therapy, MR proved more sensitive in the detection of postoperative signal intensity changes in the adjacent brain. Areas of prolonged T1 and T2 relaxation time were identified in the temporal lobes in seven of 11 cases. These changes varied from minor to extensive, involved primarily white matter, and were asymptomatic in all instances. In each case, CT demonstrated no focal abnormality. In contrast, neither MR nor CT demonstrated abnormalities in the temporal lobes of nine patients who had undergone only transsphenoidal surgery and had not received previous radiation therapy.

Areas of prolonged T1 and T2 relaxation were seen to involve the temporal lobe white matter in two of the three patients who had previously been treated with radiation ther-

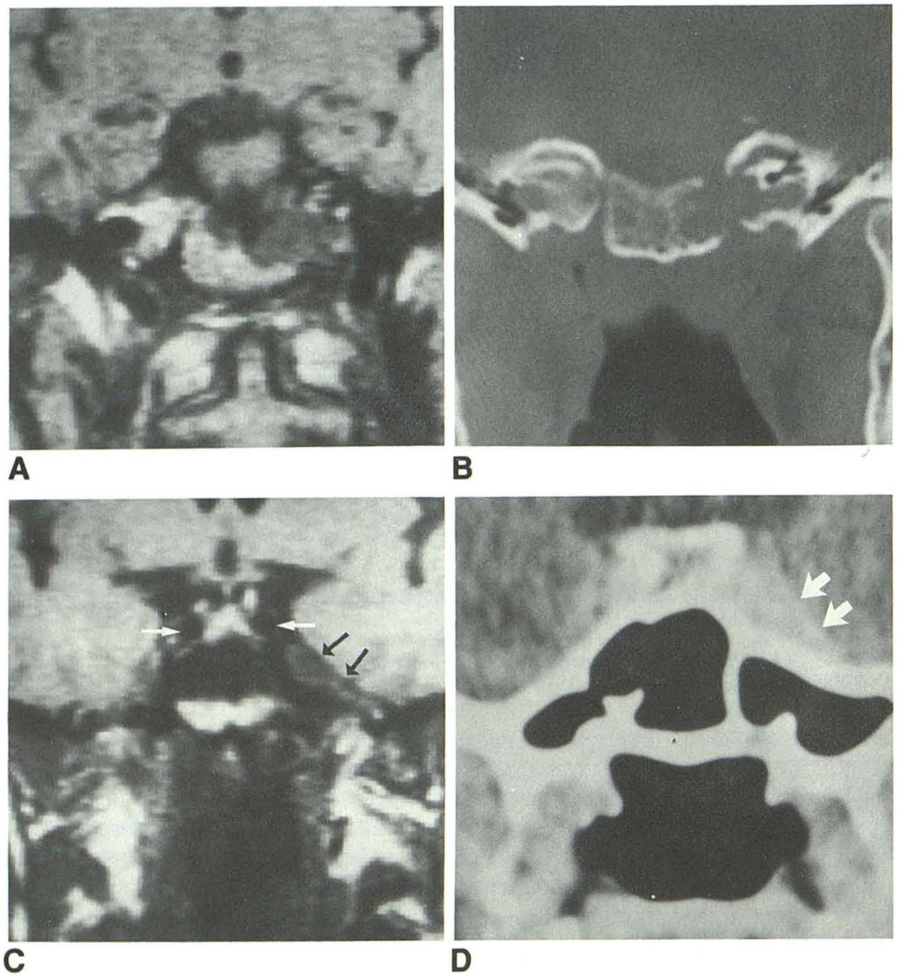

Fig. 3.—Chondrosarcoma in 59-year-old woman.

A, SE 500/30 MR image shows tumor mass involving lateral aspect of clivus.

B, Coronal CT demonstrates corresponding bone destruction.

C and *D*, SE 500/30 MR image (*C*) and coronal contrast CT scan (*D*) show subtemporal extension of tumor (*black arrows*) abutting inferolateral aspect of cavernous sinus. Note that position of cavernous carotid arteries (*white arrows*) is more apparent on MR image.

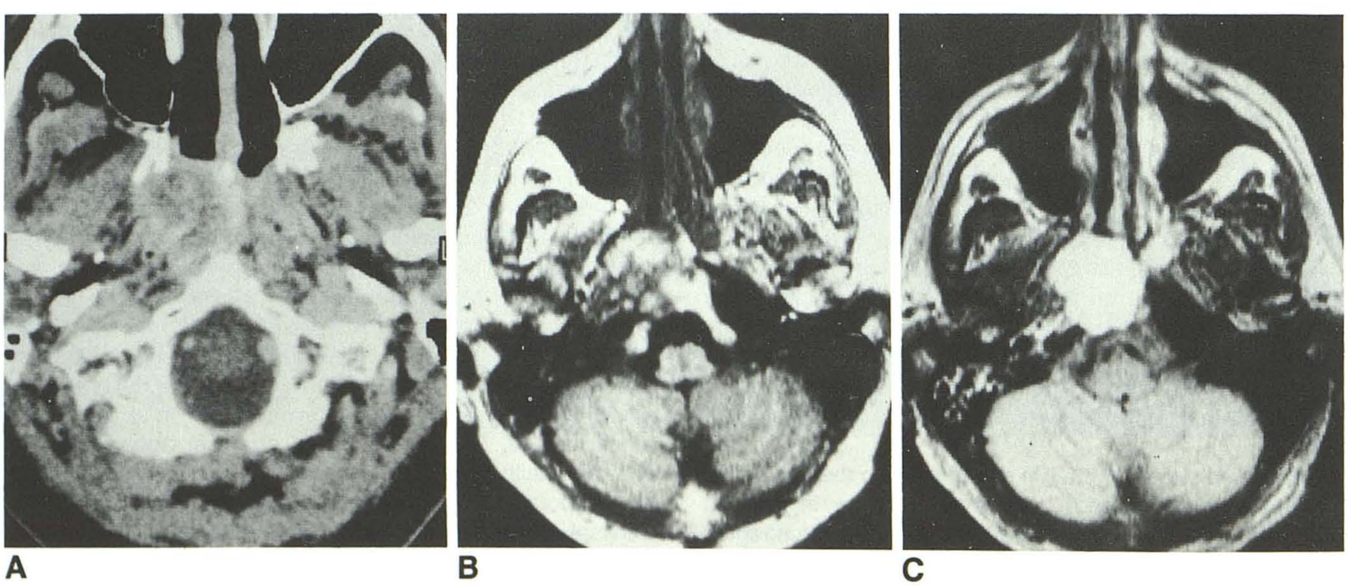

Fig. 4.—*A–C*, Nasopharyngeal extension of chondrosarcoma in 47-year-old woman. Axial postcontrast CT scan (*A*), IR 1500/450/32 MR image (*B*), and SE 2000/(60),120 MR image (*C*) accurately depict tumor involving medial and left side of nasopharynx.

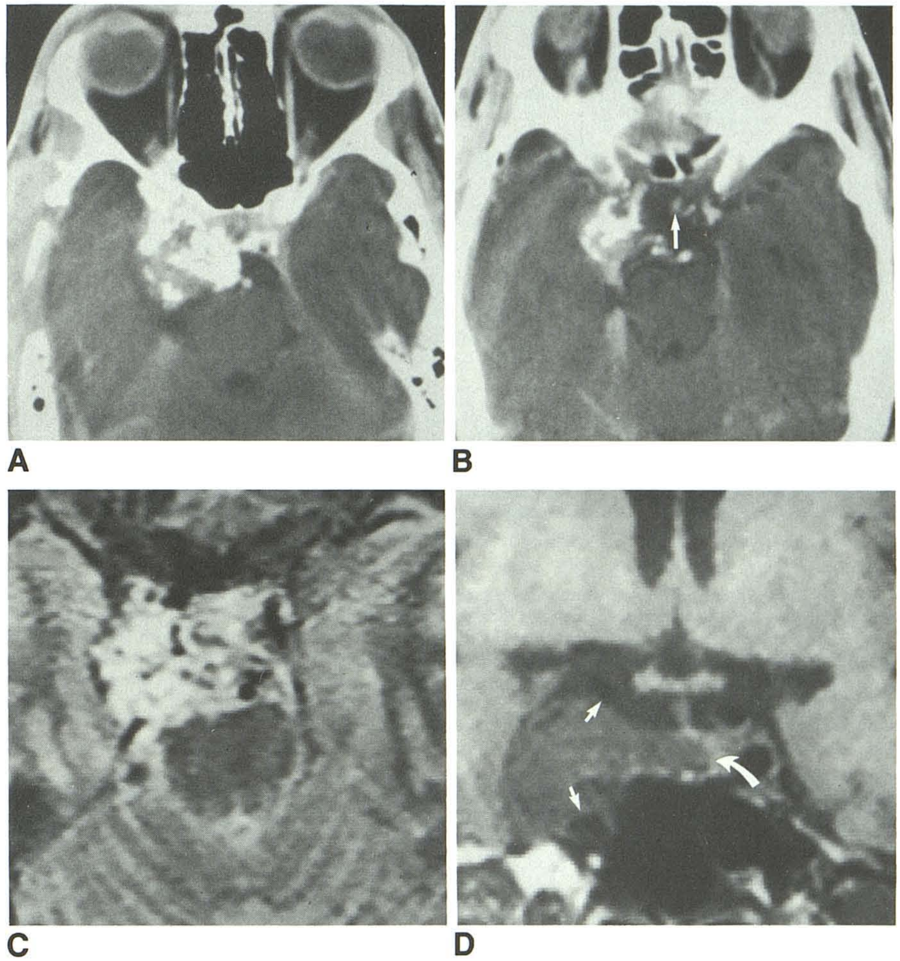

Fig. 5.—Chondrosarcoma in 41-year-old man.
A **and** ***B*****, Axial contrast CT scans show that tumor contains multiple foci of calcification. Position of cavernous internal carotid artery on right could not be determined. Note slight contralateral displacement of pituitary stalk in** ***B*** **(*****arrow*****).**
C**, SE 2000/(60),120 MR image is inferior to CT in the demonstration of calcification.**
D**, SE 500/30 MR image demonstrates displacement of carotid artery (*****straight arrows*****) and reveals extension of tumor into sella, displacing pituitary gland (*****curved arrow*****).**

apy. Both these abnormalities were clinically asymptomatic, and in one instance CT demonstrated no focal abnormality. In the second patient, IV contrast-enhanced CT demonstrated an irregular ring-enhancing focus, separate from the original lesion (Fig. 6). This temporal lobe abnormality was proved by surgical biopsy to represent coagulative necrosis, consistent with radiation effect.

CT always proved superior to MR in defining the exact nature and extent of the bone destruction caused by the tumor (Fig. 7). Similarly, it was also found to be better for demonstrating calcification within the tumor. CT revealed the presence of calcification and/or bone sequestra in 17 patients, but corresponding areas of decreased signal were seen by MR in only eight patients. The calcifications were seen as signal voids in two instances and as areas of decreased MR signal in six cases.

Discussion

The anatomic complexity of the skull base demands high-resolution imaging for the successful diagnosis and treatment of chordomas, low-grade chondrosarcomas, and other lesions of the clivus and adjacent structures. Prior to either surgery or radiation therapy, it is crucial that the relationship between the tumor mass, cranial nerves, and vital vascular structures of the skull base be accurately delineated.

CT is a proved, effective technique for studying the skull base. Thin-section scanning and appropriate field-of-view bone algorithms provide excellent bone detail. While CT is very accurate in the depiction of bone abnormalities, it is comparatively limited in its ability to depict soft-tissue structures in the posterior fossa, because of beam-hardening artifacts. In contrast to CT, cortical bone structures generate little or no signal and produce no artifact in the MR image, and these important anatomic relationships can generally be appreciated readily. The administration of subarachnoid nonionic contrast material, typically via lumbar puncture and using 4–6 ml of isotonic contrast, has been shown to greatly improve the ability of CT to discriminate these anatomic relationships [9, 10]. While generally a safe procedure, this technique is associated with some morbidity [11, 12] and is not always successful. In our experience, metrizamide CT never provided information not available in the MR images. As our experience with MR in evaluating these tumors increased, we saw that information from metrizamide CT was redundant; consequently, at this institution, this procedure is no longer generally performed for this application.

The unrestricted multiplanar capability of MR is a great

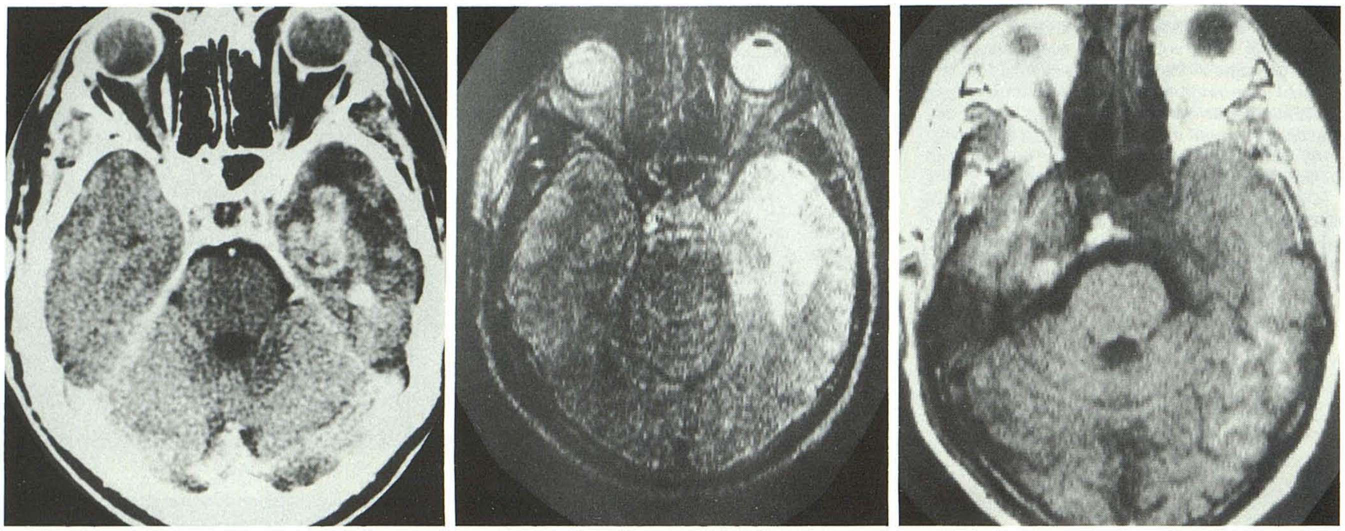

A B C

Fig. 6.—Chordoma in 57-year-old man who had been treated with 66.6 cobalt gray equivalents of proton beam irradiation 4 years earlier. There were no symptoms referable to temporal lobe. At biopsy, coagulative necrosis consistent with radiation change was encountered, with no evidence of tumor.

A, Axial postcontrast CT scan demonstrates a focus of irregular ring enhancement in left temporal lobe: enhancement is seen separate from tumor volume. Coronal images further posterior were grossly degraded by dental amalgam artifact.

B, Axial 2000/(60),120 MR image. Extensive signal intensity abnormality is seen in temporal lobe, involving white matter more than gray.

C, IR 1500/450/32 MR image. Prolonged T1 relaxation is seen in temporal lobe. It is difficult to separate this abnormality from the lateral margin of tumor volume as the signal intensity of these regions is very similar.

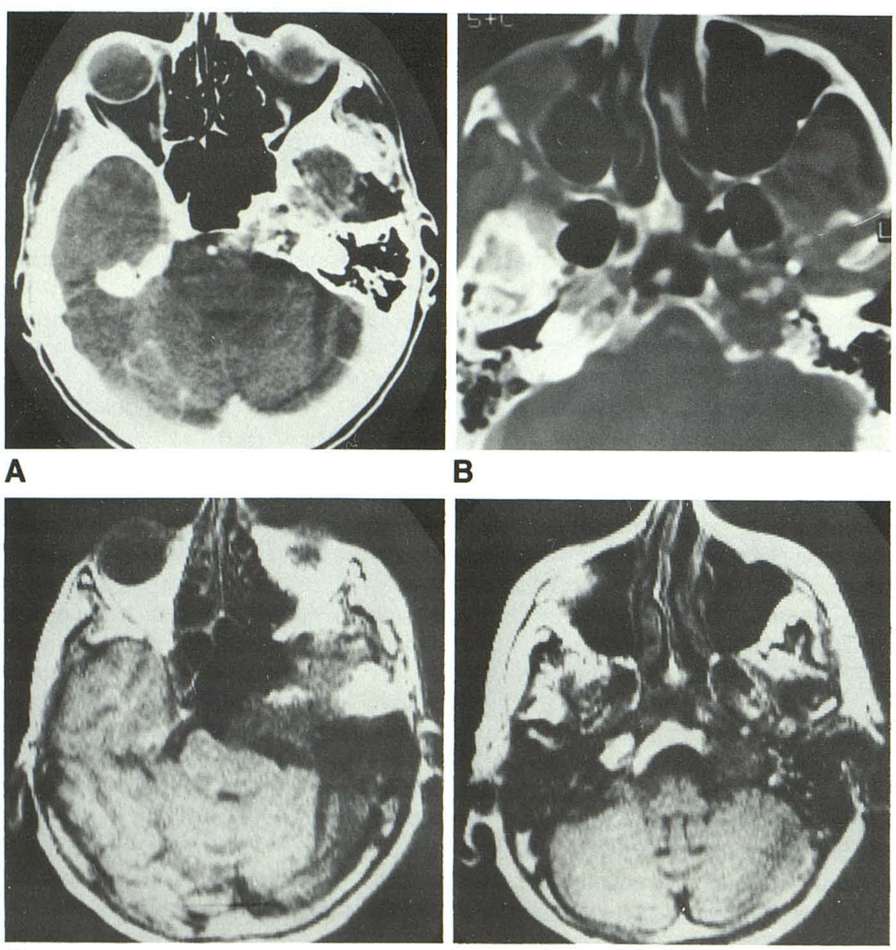

A B C D

Fig. 7.—Low-grade chondrosarcoma in 79-year-old woman.

A and *B*, Axial postcontrast CT sections depict tumor mass and accurately show bone destruction of skull base.

C and *D*, IR 1500/450/32 MR images detect tumor and demonstrate interface with brainstem as accurately as CT scan, but they are less exact in their definition of bone changes.

advantage in the staging of these tumors. Sagittal images were generally the most valuable in defining the posterior margin of the tumor, showing its relation to the neural axis and depicting nasopharyngeal extension of tumor. Coronal images were the most helpful in detecting extension of tumor into the cavernous sinus and in depicting the position of the optic chiasm and tract. While standard dental amalgam causes no artifact on MR, the presence of ferromagnetic objects, such as bridgework, may distort the magnetic field. This can cause significant image degradation [13], although this did not present a problem in any of our cases. In one instance (Fig. 8), scatter artifact from metallic but nonferromagnetic surgical clips degraded the CT scan but not the MR image in a patient who could not tolerate coronal CT.

A clear advantage of MR is its ability, in noncontrast images, to readily demonstrate patent major vessels as flow voids [14, 15]. The internal carotid and basilar arteries could be clearly discerned, and their respective positions relative to the tumor volume were reliably demonstrated. Noncontrast CT was invariably inferior in demonstrating these relationships and the use of IV contrast material was required for CT to reliably depict these structures. While CT was generally very accurate in defining the position of the intracranial vertebral and basilar arteries, it was frequently difficult to distinguish the cavernous internal carotid arteries from the high density and/or enhancement of the tumor and the cavernous sinus. The ability of MR to quantify the degree of vascular stenosis was not addressed by this study. Further work with MR systems, which will afford higher signal-to-noise and spatial resolution [16] or special pulse sequences more sensitive to flow [17, 18], may prove capable of providing this information.

While it appears clear that MR is extremely sensitive in detecting signal intensity abnormalities in patients who have had surgery and/or radiation therapy, the significance of these findings is unclear. Regions of prolonged T1 and T2 relaxation, which were clinically asymptomatic in all instances, were seen by MR in the temporal lobe white matter in the majority (seven of 11, or 78%) of patients who had undergone previous temporal craniotomies but who had not been irradiated. MR demonstrated similar signal intensity changes in two of three patients who had previously been irradiated. The high occurrence of these signal intensity variations appears to limit their differential diagnostic value. Our findings are consistent with the recent experience of Hecht-Leavitt et al. [19], who detected radiation related changes of varying degrees of severity in 58% of patients who had undergone cranial irradiation. Dooms et al. [20] also found MR to be extremely sensitive for the detection of signal intensity abnormalities in patients who had undergone previous irradiation, but they indicated that these findings were nonspecific and of little value in differentiating between residual tumor or changes due to radiation. While CT is also severely limited in its ability to make this differentiation [21, 22], information from IV contrast CT can prove useful in patient management. In one of our patients who had been previously irradiated (Fig. 6), CT demonstrated a focal enhancing abnormality. Despite the fact that MR demonstrated more extensive changes, this information was of limited value in the selection of the biopsy site. The role of contrast-enhanced MR in the assessment of these patients has not been defined. It is possible that the use of

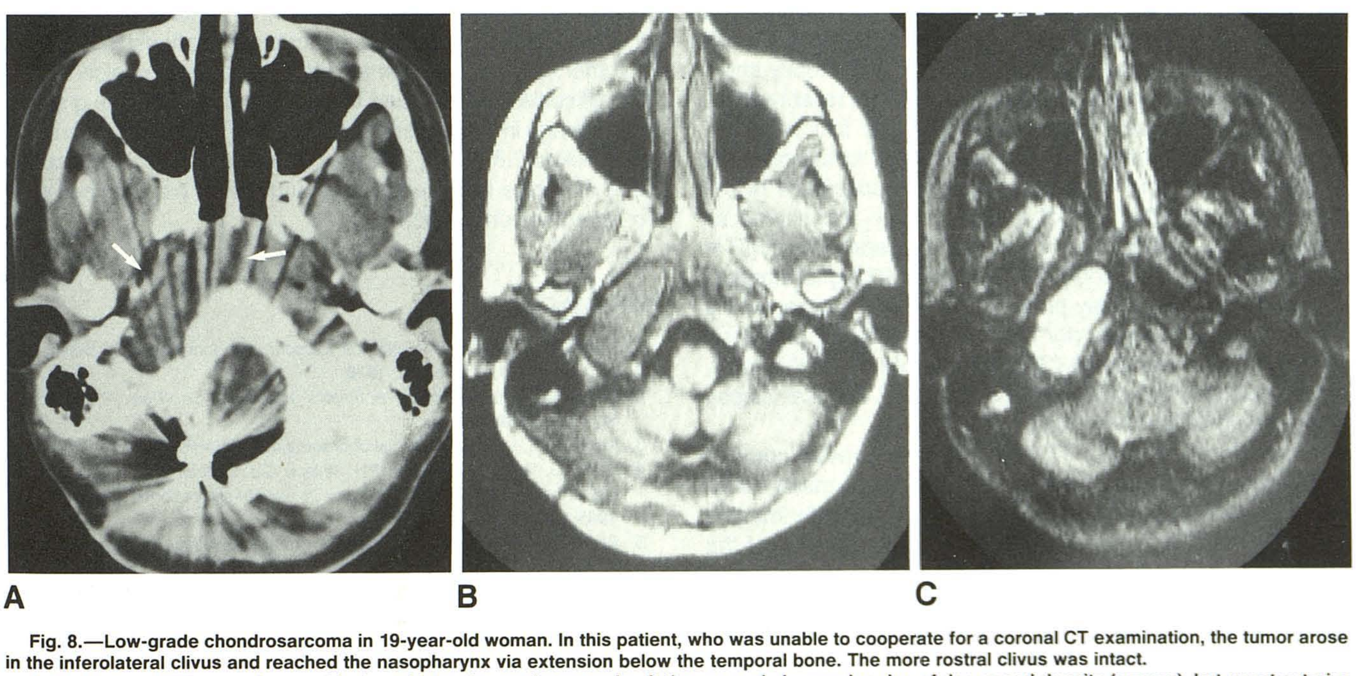

A B C

Fig. 8.—Low-grade chondrosarcoma in 19-year-old woman. In this patient, who was unable to cooperate for a coronal CT examination, the tumor arose in the inferolateral clivus and reached the nasopharynx via extension below the temporal bone. The more rostral clivus was intact.

A, Postcontrast CT scan shows widening of lateral nasopharyngeal soft tissues and abnormal region of decreased density (*arrows*), but exact anterior and medial margins of tumor are difficult to discern, in part because of the artifact introduced by the surgical clips, in this young patient with a large amount of adenoidal tissue.

B, SE 500/30 MR image accurately depicts the extent of nasopharyngeal component of this tumor. MR images at other levels confirmed that abnormality was confined to right side of nasopharynx and did not cross midline.

C, SE 2000/(60),120 MR image. The tumor, with a very prolonged T2, is seen in high contrast to adjacent normal nasopharyngeal soft tissues.

IV paramagnetic contrast material will come to play an important role in the MR evaluation of patients who have previously undergone treatment.

In our study, we did not address the issue of diagnostic specificity by either imaging technique. In our experience, we encountered no reliable imaging features that allowed for the accurate differentiation of chordoma from chondrosarcoma. While it is true that a midline location favors the diagnosis of chordoma and that a tumor located off midline, with respect to the clivus, is more likely to be a chondrosarcoma [2, 23], this finding is not specific. The exact anatomic nature of bone destruction, the presence and morphology of tumoral calcifications, and, in the case of CT, the pattern of contrast enhancement can narrow the differential diagnosis, which includes metastasis, atypical meningioma, contiguous extension of nasopharyngeal malignancies, and bone-based neoplasms of the skull base, such as plasmacytoma. The MR signal intensity characteristics of chordomas and chondrosarcomas also appear to be nonspecific, as these tumors display prolonged T1 and T2 relaxation times. In a report describing five sacrococcygeal tumors, the signal intensity characteristics of two chordomas were described as demonstrating moderately prolonged T1 and T2 relaxation times and were found to "differ significantly" from other tumors occurring at this site, suggesting that MR may permit the possibility of tumor differentiation at this location [24]. Sze et al. [25] indicated that CT and MR were approximately equivalent both in detecting chordoma and in suggesting the specific diagnosis, and they postulated that it might be possible to separate classic and chondroid subtype chordomas on the basis of calculated T1 and T2 relaxation times. Regions of relatively shortened T1 and prolonged T2 were demonstrated in five of our patients, but we felt that the histology underlying these signal intensity changes could not be readily inferred. Specifically, given that all our patients had undergone biopsy and/or subtotal resection, we believed we could not reliably differentiate between the possibilities that these foci were the result of old hemorrhage, most likely related to the previous surgical intervention, or were intrinsic characteristics of the tumor. It is possible that the use of such techniques as gradient echo sequences will increase the capability of MR in making this differentiation [26]. While the MR signal intensity pattern of the tumor may prove to be of value in narrowing the differential diagnosis (for example, making the diagnosis of meningioma less likely) [27], it is doubtful that this information will ever preclude the necessity of surgical biopsy before the initiation of therapy.

Information from both CT and MR often proved complementary in planning proton beam therapy. While major tumor margins were generally well demonstrated by both imaging methods, the superiority of MR in defining the position of the brainstem and optic chiasm and tracts relative to the tumor proved of value in defining the volume to be irradiated. This is particularly important for such a precise radiation technique as proton beam therapy. In approximately 75% of our cases, the superiority of MR in depicting the above relationships influenced the proton treatment of the patients. In addition, direct sagittal and coronal MR images were considered to be useful in planning treatment. At this institution, postoperative preradiation MR studies are now routinely obtained in all patients.

CT clearly plays a crucial role in the planning of this form of therapy since the determination of the proton radiation dose can be calculated from CT absorption coefficient measurements [28]. This is especially important in planning treatment with charged particles, since tissue inhomogeneities may significantly affect the dosage. This information is crucial in defining the compensatory gradients that are applied to the proton beam to effect the accurate delivery of the proton energy to the tumor volume. Similarly, before each treatment, the patient is placed in the same position as that used for the radiation-planning CT. This is readily achieved by using digital alignment films constructed from the CT data [29].

As both techniques proved capable of defining gross tumor margins, either CT or MR might be used for patient follow-up in most circumstances. Given its greater availability and lower cost, CT can be recommended as the technique of choice in most instances. As MR often provided superior definition of the relationship between the tumor and the posterior fossa neural axis, the optic chiasm, and the cavernous sinus, MR may provide superior information in assessing clinical symptoms believed to be caused by tumor compressing or invading these structures. There are, however, other clinical situations in which CT may prove to be the method of choice. For example, given the high occurrence and apparent nonspecificity of the signal intensity changes, as demonstrated by noncontrast MR, in the brains of patients who have had surgery and/or radiation therapy, this information may be of limited value in differentiating between residual and/or recurrent tumor and radiation effect. IV contrast-enhanced CT, while less sensitive than MR in the detection of abnormalities, may prove to be of greater utility in this context. In situations in which it is critical to define exact bone relationships relative to tumor, CT will likely remain the procedure of choice. Given the difficulties experienced to date in reliably detecting acute hemorrhage in the MR image, especially in systems operating at or below 0.6 T [30], CT may remain the diagnostic procedure of choice in the acute investigation of patients believed to have this complication.

REFERENCES

1. Dahlin DC. *Bone tumors: general aspects and data on 6,221 cases*, 3rd ed. Springfield, Ill: Thomas, **1978**
2. Wilner D. *Radiology of bone tumors and allied disorders.* Philadelphia: Saunders, **1982**
3. Kendall BE, Lee BCP. Cranial chordomas. *Br J Radiol* **1977**;50:687–698
4. Raffel C, Wright DC, Gutin PH, Wilson CB. Cranial chordomas: clinical presentation and radiation therapy in twenty-six patients. *Neurosurgery* **1985**;17:703–710
5. Pearlman AW, Friedman M. Radical radiation therapy of chordoma. *AJR* **1970**;108:333–341
6. Heffelfinger MJ, Dahlin DC, MacCarty CS, Beabout JW. Chordomas and cartilaginous tumors at the skull base. *Cancer* **1973**;32:410–420
7. Suit HD, Goitein M, Munzenrider J, et al. Definitive radiation therapy for chordoma and chondrosarcoma of base of skull and cervical spine. *J Neurosurg* **1982**;56:377–385
8. Suit H, Griffin T, Almond P, Castro J, Raju MR. Particle radiation therapy. *Cancer Treat Symp* **1984**;1:147–160
9. Steele JR, Hoffman JC. Brainstem evaluation with CT cisternography. *AJNR* **1980**;1:521–526, *AJR* **1981**;136:287–292

10. Mawad ME, Silver AJ, Hilal SK, Ganti SR. Computed tomography of the brainstem with intrathecal metrizamide. Part 1: The normal brainstem. *AJNR* **1983**;4:1–11, *AJR* **1983**;140:553–563
11. Drayer BP, Rosenbaum AE, Reigel DB, Bank WO, Deeb ZL. Metrizamide computed tomographic cisternography: pediatric applications. *Radiology* **1977**;124:349–357
12. Caille JM, Guibert-Tranier F, Howa JM, Billerey J, Calabet A, Piton J. Cerebral penetration following metrizamide myelography. *J Neuroradiol* **1980**;7:3–12
13. New PFJ, Rosen BR, Brady TJ, et al. Potential hazards and artifacts of ferromagnetic and nonferromagnetic surgical and dental devices in nuclear magnetic resonance imaging. *Radiology* **1983**;147:139–148
14. Bradley WG, Waluch V. Blood flow: magnetic resonance imaging. *Radiology* **1985**;154:443–450
15. Axel L. Blood flow effects in magnetic resonance imaging. *AJR* **1984**;143:1157–1166
16. Crooks LE, Arakawa M, Hoenninger J, McCarten B, Waits J, Kaufman L. Magnetic resonance imaging: effects of magnetic field strength. *Radiology* **1984**;151:127–133
17. Wedeen VJ, Rosen BR, Chesler D, Brady TJ. MR velocity imaging by phase display. *J Comput Assist Tomogr* **1985**;9:530–536
18. Moran PR, Moran RA, Karstaedt N. Verification and evaluation of internal flow and motion. True magnetic resonance imaging by the phase gradient modulation method. *Radiology* **1985**;154:433–441
19. Hecht-Leavitt C, Curran WJ, Zimmerman RA, et al. MRI with cranial irradiation effects. Presented at the annual meeting of the American Society of Neuroradiology, San Diego, January **1986**
20. Dooms GC, Hecht S, Brant-Zawadzki M, Berthiaume Y, Norman D, Newton TH. Brain radiation lesions: MR imaging. *Radiology* **1986**;158:149–155
21. Mikhael MA. Radiation necrosis of the brain: correlation between patters on computed tomography and dose of radiation. *J Comput Assist Tomogr* **1979**;3:241–249
22. Deck MDF. Imaging techniques in the diagnosis of radiation damage to the central nervous system. In: Gilbert HA, Kagan AR, eds. *Radiation damage to the nervous system.* New York: Raven, **1980**
23. Grossman RI, Davis KR. Cranial computed tomographic appearance of chondrosarcoma of the base of the skull. *Radiology* **1981**;141:403–408
24. Pettersson H, Hudson T, Hamlin D, et al. Magnetic resonance imaging of sacrococcygeal tumors. *Acta Radiol [Diagn] (Stockh)* **1985**;26:161–165
25. Sze GK, Uichanco LS, Brant-Zawadzki M, et al. Magnetic resonance imaging of craniocervical chordomas. Presented at the annual meeting of the American Society of Neuroradiology, San Diego, January **1986**
26. Edelman RR, Johnson K, Buxton R, et al. MR of hemorrhage: a new approach. *AJNR* **1986**;7:751–756
27. Spagnoli MS, Goldberg HI, Grossman RI, et al. Intracranial meningiomas: high-field MR imaging. *Radiology* **1986**;161:369–375
28. Goitein M. Compensation for inhomogeneities in charged particle radiotherapy using computed tomography. *Int J Radiat Oncol Biol Phys* **1978**;4:499–508
29. Goitein M, Abrams M, Rowell D, Pollari H, Wiles J. Multidimensional treatment planning: II. Beam's eye-view, back projection, and projection through CT sections. *Int J Radiat Oncol Biol Phys* **1983**;9:789–797
30. Dooms GC, Uske A, Brant-Zawadzki M, et al. Spin-echo MR imaging of intracranial hemorrhage. *Neuroradiology* **1986**;28:132–138